Effect of local magnetic field disturbances on inertial measurement units accuracy

Xavier Robert-Lachaine[1,*], Hakim Mecheri[1], Christian Larue[1] and André Plamondon[1]

[1] Institut de Recherche Robert Sauvé en Santé et en Sécurité du Travail, 505 Maisonneuve Ouest, Montréal, QC, Canada.

* Corresponding author: xavier.robert-lachaine@irsst.qc.ca

Abstract

Inertial measurement units (IMUs), a practical motion analysis technology for field acquisition, have magnetometers to improve segment orientation estimation. However, sensitivity to magnetic disturbances can affect their accuracy. The objective of this study was to determine the joint angles accuracy of IMUs under different timing of magnetic disturbances of various durations and to evaluate a few correction methods. Kinematics from 12 individuals were obtained simultaneously with an Xsens system where an Optotrak cluster acting as the reference system was affixed to each IMU. A handling task was executed under normal laboratory conditions and imposed magnetic disturbances. Joint angle RMSE was used to conduct a three-way repeated measures analysis of variance in order to contrast the following disturbance factors: duration (0, 30, 60, 120 and 240 seconds), timing (during the disturbance, directly after it and a 30-second delay after it) and axis (X, Y and Z). The highest joint angle RMSE was observed on rotations

about the Y longitudinal axis and during the longer disturbances. It stayed high directly after a disturbance, but returned close to baseline after a 30-second delay. When magnetic disturbances are experienced, waiting 30 seconds in a normal condition is recommended as a way to restore the IMUs' initial accuracy. The correction methods performed modestly or poorly in the reduction of joint angle RMSE.

Keywords: distortion; magnetometers; error; correction; compensation

Highlights (3 to 5 of 85 characters)

- The duration of a magnetic disturbance is related to the amount of error in the joint angles of IMUs.
- Rotations about the Y longitudinal axis of the joints are the most affected by magnetic disturbances.
- A 30-second delay following a magnetic disturbance is needed to restore the IMUs' baseline accuracy.

1. Introduction

Inertial measurement units (IMUs) are a promising technology for motion analysis. In comparison to most optoelectronic or electromagnetic systems, the field of acquisition is not limited, and the technology is less costly, easily portable and rapidly set up. These advantages allow field deployment of applications that were previously restricted to laboratory settings. The first generations of IMUs were composed of accelerometers and gyroscopes. Orientation of a segment was estimated by integration of the angular velocities, and position was obtained by double integration of the translational acceleration. However, noise in the gyroscopes measurements signals created a random drift affecting accuracy up to 25° after 1 min (Roetenberg et al., 2005). Accelerometers can be used to estimate the tilt angle, but gravitational acceleration is invariant in the horizontal plane, which makes accelerometers unsuitable to correct heading drift. Newer generations of IMUs have added magnetometers to compensate heading drift and improve orientation estimation. The downside is that magnetometers are sensitive to the magnetic field disturbances often created by proximity to ferromagnetic objects.

Field investigations have to deal with a wide range of settings, and adaptations for motion analysis are often unrealistic or quite cumbersome, especially in workplaces. Hence, it becomes important to understand the impact of magnetic disturbances on IMUs accuracy. A few studies have reported IMUs errors due to different contexts of magnetic field disturbances. A heading error of up to 29° was reported on IMUs in a laboratory setting near the floor (de Vries et al., 2009). Lower limb kinematics measured in a laboratory, in comparison to outdoors, yielded lower repeatability on the transverse plane of each joint and the frontal plane of the ankle (Palermo et al., 2014). IMUs placed on different

mobility aiding devices caused orientation errors of up to 35.3° depending on the type of device and the IMUs positions (Kendell and Lemaire, 2009). The RMSE between IMUs and an optoelectronic system could reach peaks of 50° near a large metal object, compared to 2.6° with no disturbance (Roetenberg et al., 2007).

Until gyroscopes measurements are substantially improved, IMUs will rely on magnetometers for orientation estimation. Several studies have shown that local magnetic disturbances can affect IMUs accuracy (de Vries et al., 2009; Kendell and Lemaire, 2009; Palermo et al., 2014; Roetenberg et al., 2007). Some correction methods or algorithms have been developed to compensate for such disturbances (Bergamini et al., 2014; Roetenberg et al., 2007). Most of the fusion algorithms such as the Kalman filter combine data from the accelerometers, gyroscopes and magnetometers to optimize the orientation estimation, while being robust to a certain extent of magnetic disturbances. However, the timing in relation to the magnetic disturbance remains unclear. Whether the error is only instantaneous when the IMUs are in proximity to the disturbance source, or whether a certain delay is needed for the fusion algorithm to restore the baseline accuracy, is debatable. In addition, the motion condition between static IMUs and dynamic IMUs during a magnetic disturbance is also unclear. Moreover, the impact of the disturbance duration on IMU accuracy has not been investigated.

Hence, the main objective of the study was to determine IMUs accuracy during imposed local magnetic disturbances. The specific objectives were to determine the effects of duration and timing of the magnetic disturbances on IMUs accuracy. The hypotheses are that longer magnetic disturbances will increase error and that a delay will be needed post-disturbance to restore baseline accuracy. The secondary objective of the study was to

evaluate a few additional correction methods designed to reduce errors due to magnetic disturbances.

2. Methods

2.1 Subjects

Prior to participation in the study, 12 healthy participants (9 men, 3 women, 26.3 ± 4.4 years, height 171.4 ± 6.8 cm and weight 74.4 ± 18.3 kg) completed a consent form approved by the Université de Sherbrooke Ethics Committee. Inclusion criteria were good physical capacity according to the Physical Activity Readiness Questionnaire (PAR-Q) and no self-reported musculoskeletal disorders during the last year. Age over 60 was the exclusion criterion.

2.2 Instrumentation

Whole-body kinematics were recorded at 30 Hz simultaneously with an 8-camera Optotrak system (Northern Digital Inc., Ontario, Canada) and a full-body Xsens system (MVN, Xsens Technologies, Enschede, Netherlands). The systems were synchronized using MVN Studio 3.5 with a trigger signal coming from the Optotrak system. The Xsens system is composed of 17 IMUs strapped over the hands, forearms, upper arms, scapulae, head, sternum, pelvis, thighs, shanks and feet (Fig. 1). When possible, sensors were placed over the bones and not the muscles to reduce soft tissue artifact (Leardini et al., 2005). A four-LED Optotrak cluster was rigidly affixed to the top of every IMU with

Velcro and tie-wrap (Fig. 1). Optotrak wires were securely attached around the waist to ensure freedom of movement and reduce load on the limbs. The Xsens IMUs were connected to each other and to two Xbus attached at the waist, which transferred the data wirelessly.

Fig. 1 – Subject setup of the full-body Xsens system with the 17 inertial measurement units (IMUs) and Optotrak clusters.

2.3 Experimental protocol

Anthropometrics including height, shoe sole height, arm span, shoulder width, foot length, ankle height, knee height, hip height and hip width were gathered for every

subject. These measurements were input into the MVN model of Xsens to estimate segment lengths with regression equations (Roetenberg et al., 2009). Afterwards, anatomical landmarks following the International Society of Biomechanics (ISB) recommendations (Wu et al., 2002; Wu et al., 2005) were identified with a probe from the Optotrak system during a standing static neutral position. To establish a relationship between sensor and segment orientation, the IMUs system was calibrated with a T-pose for the MVN model. This single posture consisted of standing straight with arms abducted to 90°, elbows extended, palms facing the ground and legs straight with feet pointing forward. The subjects were passively placed in the desired position by the operator and were asked to maintain the position for a few seconds to improve the accuracy of the calibration (Robert-Lachaine et al., 2017).

Each subject performed a trial of three repetitions of simple, short, functional movements involving each joint successively. Manual material handling tasks were performed on a rectangular aluminum platform (size 130 × 190 × 18 cm). Four stations were set up, one at each corner of the platform; the first station was 106 cm in height and the second station, opposite it, was 14 cm. These two stations were mirrored by the third and fourth stations at the other end of the platform. An empty box (size 34 × 26 × 33 cm, mass 0.5 kg) was moved from the first station to the second and then returned to the first station. A pace was imposed, with sounds indicating when to pick up and deposit the box. At the other end of the platform, a metal box (size 34 × 33 × 21 cm, mass 3.1 kg) was moved from the third to the fourth station. In addition, a metal drawer filled with ferromagnetic objects to deviate the magnetic field was placed between the third and fourth stations, in front of the subject. One side of the platform was thus a normal

laboratory condition and the other side was an imposed magnetic disturbance condition. The subjects were asked to keep pace, but no instructions were given with regards to handling technique. An indication of the range of motion for each joint during the tasks was previously described (Robert-Lachaine et al., 2016).

2.3.1 Dynamic trial

A dynamic trial was performed to measure the effects of timing, duration and axis of the magnetic disturbances, and to evaluate the correction methods. The dynamic trial was composed of intervals alternating between lifting an empty box on the normal laboratory side and lifting a metal box on the imposed magnetic disturbance side (Fig. 2). The subjects performed lift intervals alternating between the two sides of the platform as follows:

- 1 minute normal side (16 lifts)
- 30 seconds disturbance side (8 lifts)
- 1 minute normal side (16 lifts)
- 1 minute disturbance side (16 lifts)
- 1 minute normal side (16 lifts)
- 2 minutes disturbance side (32 lifts)
- 1 minute normal side (16 lifts)
- 4 minutes disturbance side (64 lifts)
- 1 minute normal side (16 lifts)

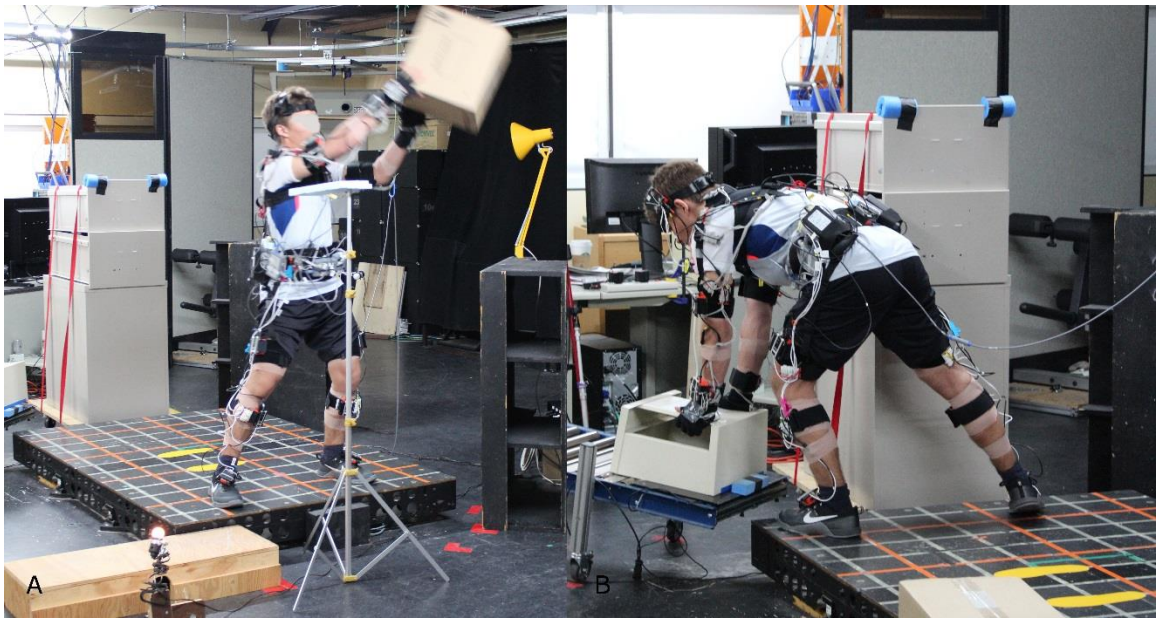

Fig. 2 – Manual material handling task performed on the normal laboratory conditions side (A) and the imposed magnetic disturbance side (B) during the dynamic trial.

2.3.2 Static trial

A static trial was conducted to determine IMUs accuracy while the subject remained static near the magnetic disturbance and to evaluate the correction methods under this condition. A large metal chair was placed close to the metal drawer. The subject started by lifting the empty box for one minute on the normal side. Then, the subject sat on the chair while staying close to the drawer and remained static for four minutes (Fig 3). Finally, the subject repeated the 16 lifts during 1 minute on the normal side.

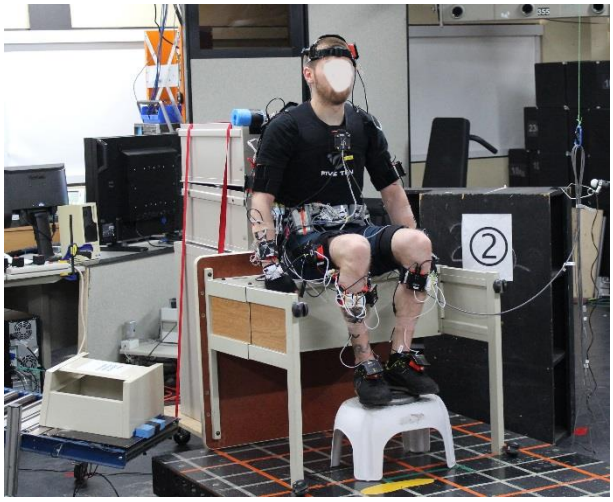

Fig. 3 – Experimental setup and posture maintained by the subjects during the imposed magnetic disturbance static trial.

2.4 Biomechanical model

Two segmental biomechanical models were used with the two systems as in recent studies (Robert-Lachaine et al., 2016, 2017). First, the ISB model was based on anatomical landmarks as per the ISB recommendations (Wu et al., 2002; Wu et al., 2005). Joint centers were defined according to the ISB guidelines. More specifically, the hip joint center of rotation was estimated with a predictive approach using pelvic width, pelvic depth and leg length (Harrington et al., 2007) as suggested in a systematic review (Kainz et al., 2015). Arm flexion/extension, abduction/adduction and circumductions were executed to determine the functional glenohumeral joint center (Gamage and Lasenby, 2002). Finally, the cervical center of rotation was estimated with a predictive approach relying on incisura jugularis and C7 anatomical landmarks (Reed et al., 1999).

Anatomical coordinate systems were built according to the CAST protocol (Cappozzo et al., 1995).

The second biomechanical model, MVN, is provided by the Xsens IMUs system. It defines segment lengths with regression equations based on the anthropometric measures (Roetenberg et al., 2009). The calibration was done while the subject maintained a specific static posture where the relationship between each IMU and segment orientation was established (Roetenberg et al., 2009). The posture was the T-pose, and the subject was passively placed by the operator to increase calibration accuracy and similarity to laboratory motion analysis (Robert-Lachaine et al., 2017). Afterwards, segment orientation was estimated using the Kalman filter fusion algorithm. Since the MVN model separates the spine into multiple sections, the relative quaternion was used to calculate joint angles between the head orientation and thorax orientation for the neck joint and between the pelvis orientation and thorax orientation for the back joint.

2.5 Data analysis

To compare IMUs data to optoelectronic system data, the local coordinate systems of each segment must be aligned. Angular velocities were used during simple, short, functional movements to align the local coordinate systems from the two systems (de Vries et al., 2009), because this method was the recommended amongst eight methods (Mecheri et al., 2016).

In the ISB model, the anatomical coordinate systems were defined according to the identified anatomical landmarks as per the ISB recommendations (Wu et al., 2002; Wu et

al., 2005) relative to the fixed clusters on each segment. The same transformation matrices were applied to the IMUs to orient them according to the anatomical landmarks and the ISB model. Joint angles were calculated from the segment orientations following the Z-X-Y sequence of Euler angles with the exception of the shoulder, which used the X-Z-Y sequence. As in a recent study (Robert-Lachaine et al., 2016), joint angles from the Optotrak and IMUs systems, both using the same ISB model, were compared (with the optoelectronic system serving as reference) in order to isolate only the "technological error" component. The correspondence between functional movements and rotation about each axis of the joints is described in Table 1.

Table 1 Correspondence between functional movements and rotations about the Z, X and Y axes for all joints.

Joint	Z axis	X axis	Y axis
Wrist	Flexion/Extension	Ulnar deviation	Pronation/Supination
Elbow	Flexion/Extension	Carrying angle	Pronation/Supination
Shoulder	Flexion/Extension	Adduction/Abduction	Axial rotation
Neck	Flexion/Extension	Lateral rotation	Axial rotation
Back	Flexion/Extension	Lateral rotation	Axial rotation
Ankle	Dorsiflexion/Plantarflexion	Inversion/Eversion	Axial rotation
Knee	Flexion/Extension	Varus/Valgus	Axial rotation
Hip	Flexion/Extension	Adduction/Abduction	Axial rotation

Joint angle differences were assessed with root mean square error (RMSE). Joint angle RMSE was calculated for each disturbance interval, which varied in duration. The one-minute intervals under the normal laboratory conditions were separated into two sections corresponding to the first and last 30 seconds, and the joint angle RMSE was calculated for each. The **timing** was represented by the joint angle RMSE measured **during** the disturbance, directly **after** it (0 to 30 seconds after the disturbance) and with a 30-second **delay** (30 to 60 seconds after the disturbance). The **duration** was represented by the

length of the magnetic disturbances: 0, 30, 60, 120 and 240 seconds, where 0 seconds corresponds to the baseline accuracy of the IMUs under normal laboratory conditions. To indicate the amount of imposed magnetic disturbance, the variation in the magnetic norm (|M|) was measured for each condition. A normalized magnetic norm (% |M|) was calculated from the absolute difference between the measured magnetic norm ($|M|_m$) and the initial magnetic norm obtained during the first two seconds on the normal laboratory side ($|M|_i$):

$$\% \, |\mathrm{M}| = 100 * \frac{abs(|\mathrm{M}|_m - \ |\mathrm{M}|_i)}{|\mathrm{M}|_i} \qquad (1)$$

The mean and SD of the % |M| were calculated over the period of each timing (during, after, delay) and duration.

Three additional correction methods, available in the MVN commercial software, were tested:

- Kinematic algorithm coupling (KiC)
- Kinematic algorithm (KiC2)
- Reset orientation filter (reset)

The first method, called kinematic algorithm coupling (KiC), is based on the assumption that two segments are coupled by a joint. The algorithm supplies the relative orientation between two segments without using any assumptions about the local magnetic field during movements. The magnetometers are used to provide stability around the global vertical axis when there is no motion. The second method, called kinematic algorithm coupling without magnetometers (KiC2), ignores the magnetometers data at all times.

KiC and KiC2 were used on the entire trial instead of the Kalman filter. The third method, called reset orientation filter, performs a full reset of the fusion algorithm at the selected frame. The fusion algorithm builds up history to help in the estimation of the orientation; this method can be used when the IMUs have been in a magnetically distorted area for a long time. It was applied at the instant when the subject arrived on the normal side and made a small pause of two seconds after completing the lifting tasks on the disturbed side. A condition with no additional correction method (called "none") corresponding to the Kalman filter fusion algorithm was used for comparison purposes. Since KiC and KiC2 were only developed for the lower limb joints, the analysis of the correction methods focused on the hip, knee and ankle joints. In addition, to focus on the highest errors and highest potential correction, rotations about the Y longitudinal axis, which corresponds to the vertical axis for most of the segments in a standing position affected by the heading error, were used for this analysis. Similar to the previous analysis, joint angle RMSE was calculated for each correction method and each timing and duration condition.

Bilateral joint measurements were pooled, since no apparent differences were observed between the right and left sides (Kim and Nussbaum, 2013; Robert-Lachaine et al., 2016). The Box-Cox transformation was used on the RMSE values to improve the normality of distribution and equality of variance between comparisons according to Shapiro-Wilk and Levene's tests respectively. Joint angle RMSE during the manual material handling tasks was used to conduct separate three-way repeated measures analysis of variance (ANOVA) applied to the eight joints and to contrast the factors of duration (0, 30, 60, 120 and 240 seconds), timing (**during** the disturbance, directly **after**

it, and with a 30-second **delay** after it) and axis (X, Y and Z). This analysis focuses on the main effects of duration, timing and axis, and the interaction between duration and timing.

Separate one-way repeated measures ANOVAs, applied to joint angle RSME about the Y longitudinal axis of the lower limb joints, were conducted to contrast the correction method factor (none, KiC1, KiC2, reset filter). Bonferroni post-hoc tests were conducted when a significant main effect was present to identify where the differences occurred. The significance level was set a priori to $\alpha = .05$ for all statistical analyses. Sphericity was verified with Mauchly's test and, when not met, the Greenhouse-Geisser correction was used.

3. Results

Magnetic norm variation (% |M|) measured during the dynamic magnetic disturbance trial (Table 2) and the static magnetic disturbance trial (Table 3) indicated the amount of magnetic disturbance sustained on average for each IMU over the period of each timing (during, after, delay). As expected, the laboratory setup affected the magnetometers on the disturbed side (during), while their values were more stable on the normal laboratory side (after and delay). The mean range of |M| reached during the dynamic trial was highest on the hand at 0.934 and lowest on the pelvis at 0.169.

Table 2 Normalized magnetic norm variation (% |M|) presented in mean percentage (SD) for each IMU and each timing and duration condition during the dynamic magnetic disturbance trial.

		Duration				
IMU	Timing	0 seconds	30 seconds	60 seconds	120 seconds	240 seconds
Hand	During	1.5 (0.6)	20.4 (4.4)	20.4 (5.2)	20.0 (4.5)	20.6 (7.1)
	After	1.1 (0.8)	1.5 (0.7)	1.5 (0.7)	1.5 (0.7)	1.9 (0.8)
	Delay	2.1 (0.7)	2.0 (0.7)	2.1 (0.8)	2.1 (0.8)	1.4 (0.7)
Forearm	During	1.1 (0.6)	13.9 (3.2)	14.3 (4.1)	13.9 (3.3)	14.2 (3.9)
	After	0.8 (0.5)	1.1 (0.6)	1.2 (0.6)	1.2 (0.6)	1.4 (0.6)
	Delay	1.5 (0.6)	1.5 (0.6)	1.5 (0.6)	1.5 (0.6)	1.1 (0.5)
Upper arm	During	1.5 (0.5)	6.5 (1.1)	6.2 (1.1)	6.4 (1.2)	6.4 (1.2)
	After	0.9 (0.3)	1.2 (0.3)	1.2 (0.4)	1.2 (0.4)	1.5 (0.5)
	Delay	1.3 (0.4)	1.5 (0.4)	1.6 (0.4)	1.6 (0.5)	1.1 (0.4)
Head	During	2.2 (0.7)	3.4 (0.4)	3.4 (0.4)	3.5 (0.3)	3.5 (0.4)
	After	1.2 (0.4)	1.7 (0.5)	1.7 (0.5)	1.7 (0.5)	2.3 (0.7)
	Delay	1.6 (0.5)	2.2 (0.6)	2.3 (0.7)	2.3 (0.7)	1.6 (0.5)
Scapula	During	0.7 (0.3)	4.1 (0.9)	3.8 (1.1)	3.8 (1.0)	3.7 (1.0)
	After	0.9 (0.3)	1.0 (0.3)	1.1 (0.3)	1.1 (0.3)	1.3 (0.4)
	Delay	1.3 (0.4)	1.3 (0.4)	1.4 (0.4)	1.4 (0.4)	1.0 (0.3)
Thorax	During	1.5 (0.6)	4.7 (0.6)	4.6 (0.8)	4.8 (0.7)	4.7 (0.6)
	After	1.0 (0.4)	1.4 (0.5)	1.5 (0.5)	1.4 (0.5)	1.9 (0.7)
	Delay	1.9 (0.7)	1.9 (0.6)	1.9 (0.7)	2.0 (0.6)	1.3 (0.5)
Pelvis	During	1.3 (0.4)	9.3 (1.6)	9.6 (1.7)	9.8 (1.7)	9.6 (1.6)
	After	0.6 (0.2)	0.8 (0.2)	0.8 (0.2)	0.8 (0.2)	1.1 (0.3)
	Delay	0.9 (0.3)	1.1 (0.4)	1.1 (0.4)	1.1 (0.4)	0.8 (0.2)
Foot	During	1.4 (0.4)	3.5 (1.1)	3.8 (1.0)	4.1 (1.3)	4.1 (1.5)
	After	0.9 (0.3)	1.3 (0.4)	1.4 (0.4)	1.3 (0.4)	1.7 (0.5)
	Delay	1.7 (0.5)	1.6 (0.5)	1.6 (0.5)	1.6 (0.5)	1.2 (0.5)
Lower leg	During	0.4 (0.3)	3.2 (1.7)	3.6 (1.7)	4.1 (1.3)	4.3 (1.7)
	After	0.7 (0.4)	0.6 (0.4)	0.5 (0.3)	0.6 (0.3)	0.7 (0.3)
	Delay	0.6 (0.4)	0.7 (0.3)	0.7 (0.4)	0.7 (0.3)	0.5 (0.3)
Upper leg	During	0.7 (0.4)	7.8 (1.7)	7.8 (2.0)	8.0 (2.3)	7.9 (2.4)
	After	0.5 (0.4)	0.6 (0.4)	0.6 (0.4)	0.7 (0.4)	0.8 (0.4)
	Delay	0.9 (0.4)	0.8 (0.4)	0.8 (0.4)	0.8 (0.4)	0.6 (0.4)

Table 3 Normalized magnetic norm variation (% |M|) presented in mean percentage (SD) for each IMU and each timing condition during the static magnetic disturbance trial.

	Timing			
IMU	Before	During	After	Delay
Hand	1.7 (0.6)	52.2 (14.9)	3.9 (1.5)	1.7 (0.6)
Forearm	0.9 (0.3)	39.2 (7.4)	2.4 (1.0)	1.0 (0.3)
Upper arm	0.9 (0.2)	9.6 (2.7)	1.5 (0.5)	0.9 (0.3)
Head	1.3 (0.5)	5.8 (1.2)	1.7 (0.7)	1.2 (0.4)
Scapula	0.8 (0.3)	20.1 (10.3)	1.3 (0.6)	0.8 (0.3)
Thorax	1.0 (0.4)	0.8 (0.7)	1.2 (0.6)	0.9 (0.4)
Pelvis	1.0 (0.2)	27.5 (21.4)	1.9 (1.1)	0.9 (0.3)
Foot	1.0 (0.4)	14.2 (3.7)	2.3 (0.9)	1.2 (0.5)
Lower leg	0.8 (0.6)	13.0 (2.4)	2.0 (0.7)	0.9 (0.6)
Upper leg	0.8 (0.3)	19.3 (7.3)	1.9 (0.8)	0.9 (0.4)

Duration, timing and axis significant main effects were observed on most of the joints and significant interactions between duration and timing were observed on all joints (Table 4). In terms of duration, longer magnetic field disturbances increased the joint angle RMSE with mean ± SD of 2.3 ± 1.0°, 3.3 ± 1.8°, 3.7 ± 2.7°, 4.2 ± 3.7°, 4.5 ± 3.9° on pooled joints, axes and timing conditions for the 0, 30, 60, 120 and 240 second conditions respectively. As for timing, the joint angle RMSE was highest during the disturbance and remained high directly after the disturbance, but returned close to baseline accuracy after a 30-second delay. The mean ± SD on pooled joints, axes and duration conditions for the timing factor was 4.7 ± 4.0° during the disturbance, 3.5 ± 2.5° after the disturbance and 2.7 ± 1.1° after a 30-second delay. For the axis factor, rotations about the Y longitudinal axis were the most affected by disturbances, with joint angle RMSE mean ± SD of 5.4 ± 4.0° on pooled joints, duration conditions and timing conditions, compared to 2.5 ± 1.2° and 3.0 ± 1.7° on rotations about the X frontal and Z transverse axes respectively. The interaction between duration and timing can be observed in Fig. 4 where the joint angle RMSE remains near the baseline level for the 30-second delay condition, but increases gradually with duration for both the during

disturbance and after disturbance conditions, but the effect is more pronounced for the during condition.

Correction method significant main effects were observed on all lower limb joints during the dynamic magnetic disturbances (Table 5). Post-hoc tests revealed that the kinematic coupling algorithm without magnetometers (KiC2) increased the knee and hip RMSE in comparison to no additional correction applied (Fig. 5). The reset orientation filter also increased the knee RMSE. In contrast, the kinematic coupling algorithm (KiC) reduced the ankle RMSE in comparison to no additional correction applied or other correction methods (Fig. 5). The correction methods joint angle RMSE mean ± SD calculated on pooled joints, duration conditions and timing conditions were 8.0 ± 2.2° for none, 7.1 ± 2.2° for KiC, 23.2 ± 8.3° for KiC2 and 9.6 ± 3.2° for the reset.

A main effect of correction method was observed on three lower limb joints during the static magnetic disturbance (Table 6). Post-hoc tests showed that the joint angle RMSE significantly increased with KiC2 compared to the other methods for the ankle and knee and that the reset method significantly reduced the joint angle RMSE compared to other methods for the hip, especially for the after and delay timing conditions (Fig 6).

Table 4 – Statistics from the separate three-way repeated-measure ANOVAs applied to joint angle RMSE to contrast the duration (0, 30, 60, 120 and 240 seconds), timing (during, directly after and with a 30-second delay) and axis factors (X, Y and Z). Significance ($P \leq .05$) is identified in bold.

	Duration		Timing		Axis		Duration × Timing	
Joint	$F_{4, 44}$	*P* Value	$F_{2, 22}$	*P* value	$F_{2, 22}$	*P* value	$F_{8, 88}$	*P* value
Wrist	23.05	**<.001**	44.47	**<.001**	23.48	**<.001**	19.07	**<.001**
Elbow	4.54	.051	73.41	**<.001**	12.41	**.003**	17.40	**<.001**
Shoulder	1.94	.191	40.05	**<.001**	.90	.371	6.45	**.008**
Neck	5.74	**.009**	12.32	**.002**	66.93	**<.001**	17.20	**<.001**
Back	0.53	.631	2.68	.125	77.89	**<.001**	5.40	**.009**
Ankle	24.28	**<.001**	76.58	**<.001**	79.42	**<.001**	17.89	**<.001**
Knee	13.69	**<.001**	45.74	**<.001**	58.17	**<.001**	9.83	**<.001**
Hip	14.73	**<.001**	22.66	**<.001**	88.75	**<.001**	14.86	**<.001**

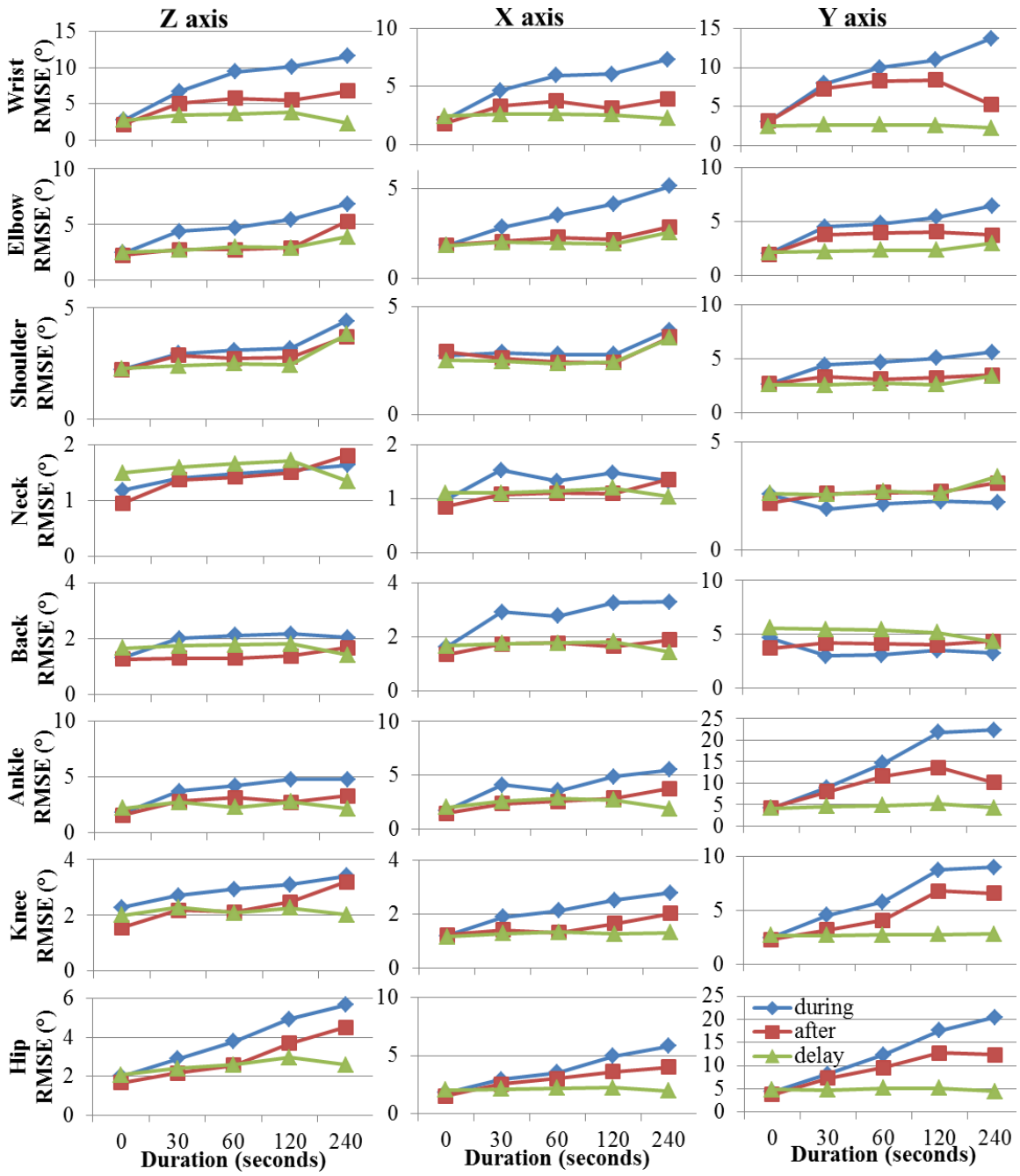

Fig. 4 – Mean joint angle RMSE measured on the eight joints and three axes during the 0, 30, 60, 120 and 240 seconds of magnetic disturbance (blue diamonds), following the magnetic disturbance (red squares) and after a 30-second delay (green triangles).

Table 5 – Statistics from the separate one-way repeated measures ANOVAs applied to joint angle RMSE about the Y axis of lower limb joints and pooled duration and timing conditions during dynamic magnetic disturbances to contrast the correction factor (none, KiC, KiC2 and reset filter) and Bonferroni post-hoc test values. Significance ($P \leq .05$) is identified in bold and a significant increase in RMSE compared to the condition "none" is underlined in the post-hoc tests.

Joint	Correction		Post hoc tests (*P* value)					
	$F_{3, 33}$	*P* value	none vs KiC	none vs KiC2	none vs reset	KiC vs KiC2	KiC vs reset	KiC2 vs reset
Ankle	11.82	**<.001**	**.014**	.919	.201	**<.001**	**.002**	>.999
Knee	53.36	**<.001**	>.999	**<u>.001</u>**	**<u>.007</u>**	**<.001**	.700	**<.001**
Hip	44.33	**<.001**	>.999	**<u>.001</u>**	.161	**<.001**	>.999	**<.001**

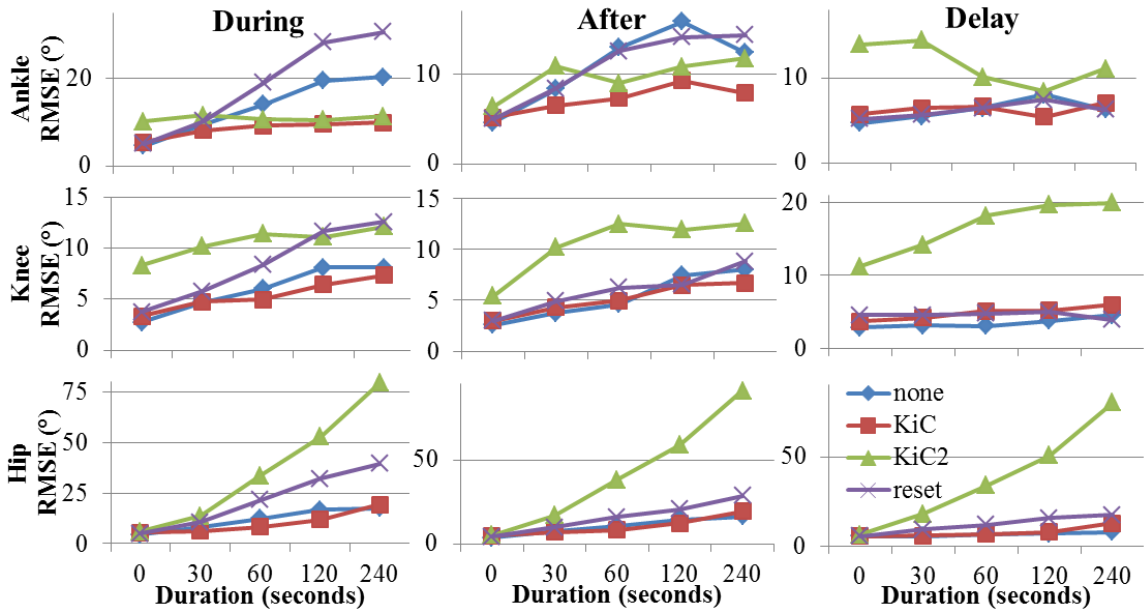

Fig. 5 – Mean joint angle RMSE about the Y axis of the lower limb joints during the 0, 30, 60, 120 and 240 seconds of dynamic magnetic disturbance (During), during the 30 seconds following the magnetic disturbance (After) and during the 30 seconds after a 30-

second delay (Delay) for four magnetic disturbance correction conditions: none (blue diamonds), kinematic coupling algorithm (red squares), kinematic coupling algorithm without magnetometers (green triangles) and reset orientation filter (purple X).

Table 6 – Statistics from the separate one-way repeated measures ANOVAs applied to joint angle RMSE about the Y axis of the lower limb joints and pooled timing conditions during static magnetic disturbance to contrast the correction factor (none, KiC, KiC2 and reset filter) and Bonferroni post-hoc test values. Significance ($P \leq .05$) is identified in bold and a significant increase in RMSE compared to the condition "none" is underlined in the post-hoc tests.

Joint	Correction		Post-hoc tests (*P* value)					
	$F_{3, 33}$	*P* value	none vs KiC	none vs KiC2	none vs reset	KiC vs KiC2	KiC vs reset	KiC2 vs reset
Ankle	13.90	**<.001**	>.999	**.017**	>.999	**.008**	>.999	**.029**
Knee	18.65	**<.001**	.671	**.006**	>.999	**.008**	>.999	**.007**
Hip	148.28	**<.001**	.413	.097	**<.001**	**.033**	**<.001**	**<.001**

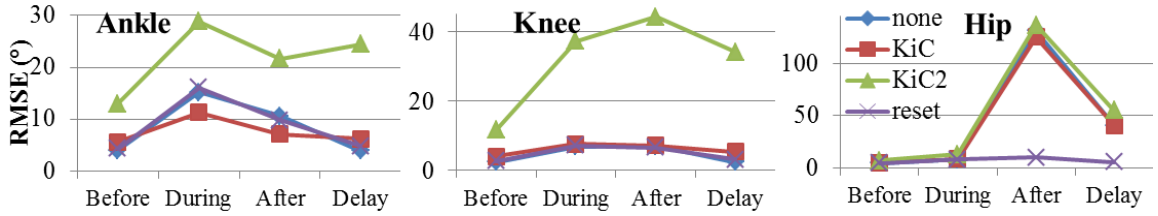

Fig. 6 – Mean joint angle RMSE about the Y axis of the lower limb joints before the magnetic disturbance (Before), during a 4-minute static magnetic disturbance with the subject seated (During), during the 30 seconds following the magnetic disturbance (After) and during the 30 seconds after a 30-second delay (Delay) for four magnetic disturbance correction conditions: none (blue diamonds), kinematic coupling algorithm (red squares), kinematic coupling algorithm without magnetometers (green triangles) and reset orientation filter (purple X).

4. Discussion

The impact of imposed local magnetic disturbances on the accuracy of IMUs was measured for conditions of duration, timing and axis during manual material handling. Rotations about the Y longitudinal axis of the joints representing the vertical axis of the majority of the segments while the subject was standing yielded higher joint angle RMSE, while the duration of the magnetic disturbance was related to joint angle RMSE increases. Joint angle RMSE was higher during the magnetic disturbance, especially for upper and lower limbs, which obtained higher %|M| but remained high directly afterward and returned to near-baseline without magnetic disturbance after a 30-second delay. A few correction methods were evaluated on rotations about the Y longitudinal axis on the lower limb during dynamic and static disturbance conditions. The KiC algorithm reduced ankle RMSE during dynamic magnetic disturbances, while the reset filter reduced the hip RMSE after the long static magnetic disturbance.

4.1 Duration

The duration of trials under normal laboratory conditions has been shown to increase IMU error (Bergamini et al., 2014; Lebel et al., 2015; Plamondon et al., 2007; Robert-Lachaine et al., 2016). However, the extent of the increase in joint angle RMSE observed from 30 seconds to 60 seconds of magnetic disturbance shows that this effect is much more pronounced during magnetic disturbances. In general, a constant progression of the joint angle RMSE was observed as the duration of the magnetic disturbance increased,

both for during and after magnetic disturbance timing conditions. There was a tendency to stabilization of the joint angle RMSE between 120 and 240 seconds of magnetic disturbance especially for the lower limb, although accuracy for even longer dynamic magnetic disturbances remains unknown.

4.2 Timing

The amount of error relative to the occurrence of the magnetic disturbance is important for field acquisition, and this aspect has not been previously investigated. As expected, our data demonstrated a higher joint angle RMSE during a magnetic disturbance than before or after. Upper and lower limbs closer to the disturbance were more affected. Neck, back and shoulder joints showed less error during the disturbance, because the IMUs on the pelvis, scapulae and head were placed caudally and sustained less %|M|, while the ferromagnetic objects were placed in front of the subject for the dynamic trial. Joint angle RMSE decreased directly after the magnetic disturbance, but stayed higher than the initial baseline. After a 30-second delay following the dynamic magnetic disturbance, accuracy was close to the initial level for all durations. However, a 30-second delay was not sufficient to restore baseline accuracy for the hip following a long static magnetic disturbance. This timing information may be useful for practical applications where the subject must be in an environment with magnetic disturbances. It could help to understand when the data can be analyzed with confidence or not and to adapt research protocols by allowing for delays after long magnetic disturbances.

4.3 Axis

Rotations about the Y axis, which represents the segment longitudinal axis or the vertical axis in a standing position especially for the lower limbs, showed the highest joint angle errors as previously reported under normal laboratory conditions (Faber et al., 2013; Plamondon et al., 2007; Robert-Lachaine et al., 2016). These results are in accordance with a previous study observing more error due to magnetic disturbance on the transverse plane (Palermo et al., 2014). Similarly, the heading angle has often been reported as the highest error due to gyroscopic drift (Bergamini et al., 2014; Schiefer et al., 2014). Since the subjects were standing and executing manual material handling tasks, the Y axis from the joints is more often exposed to the loss of magnetic north by the magnetometers, and we must then rely on gyroscopes to estimate orientation.

4.4 Correction methods

The different correction methods tested to compensate error due to magnetic disturbances have shown modest to poor results. In general, they were able to reduce the joint angle RMSE only for specific joints and conditions. KiC2, however, performed poorly: it significantly increased the joint angle RMSE for all joints and conditions. The reset orientation filter reduced the hip RMSE after static magnetic disturbances, but increased the hip, knee and ankle RMSE during dynamic magnetic disturbances. Its use may be considered after a long static magnetic disturbance, but it is not an appropriate correction method for all conditions. KiC was the most consistent method for reducing joint angle RMSE, especially for the ankle during and after magnetic disturbances. However, this

latter method did not reduce the large error occurring after long static magnetic disturbances. It must be noted that the Kalman filter condition was considered as the default or no additional correction method ("none" condition), although this fusion algorithm also helps reduce error due to magnetic disturbances (Bergamini et al., 2014). The zero points method (short break), which provides additional heading and gyroscope bias information, combined with bidirectional orientation computation (forward and backward in time), remains a relevant approach in the context of magnetic disturbance (Schiefer et al., 2014). Therefore, more effort is still needed in the development of robust correction methods capable of reducing error due to magnetic disturbances on all joints and for various conditions representative of field applications.

4.5 Limitations

The scope of the study has some limitations. The magnetic disturbances applied to the IMU system are specific to conditions in the laboratory in terms of the ferromagnetic objects used and their proximity to each IMU. No magnetic field was generated; therefore, in the presence of electric tools or motors, the results could be different. Consequently, magnetic disturbances experienced in the field or in other settings may affect IMUs differently. The results are specific to the Xsens system, and newer systems may already have better compensation algorithms for magnetic disturbances.

4.6 Field application

During field acquisition, magnetic disturbances should be avoided if possible. However, when conducting analyses in workplaces (Alvarez et al., 2015; Labaj et al., 2016; Ohlendorf et al., 2015; Prairie and Corbeil, 2014; Schall et al., 2015), this may be unrealistic. Alternative solutions must be explored for data collection and analysis. Our results indicate that a 30-second delay restored IMUs to baseline accuracy after dynamic magnetic disturbances. While this is only a minimum, a longer delay would not likely provide greater accuracy. From our recent field experience with manual material handlers, magnetic disturbances were problematic when they were driving a pallet truck. The protocol was modified to introduce some delays when workers stepped out of the pallet truck, which improved the accuracy of the IMUs when the workers were lifting boxes. For future field applications, the management of large datasets will be a challenge. The development of automation procedures will be crucial to detect portions of the data affected by magnetic disturbances.

5. Conclusions

Using kinematics obtained with IMUs and an optoelectronic system as a reference, we intended to determine the accuracy of IMUs under different timing of magnetic disturbances of various durations. The hypotheses that the duration of a magnetic disturbance was associated with the amount of error and that a delay was needed after a disturbance to restore baseline accuracy were confirmed. The accuracy of the IMUs was most affected by magnetic disturbances on rotations about the Y axis and of longer

duration. A 30-second delay following a disturbance proved effective in restoring baseline accuracy. In addition, a few correction methods designed to reduce error due to magnetic disturbances were tested; these performed poorly or modestly and were not robust to different conditions of disturbance.

Acknowledgements

The authors are grateful for the technical assistance provided by Sophie Bellefeuille.

Funding: This work was supported by the Institut de Recherche Robert-Sauvé en Santé et en Sécurité du Travail (IRSST) [grant number 2012-0040] and the IRSST postdoctoral scholarship program.

References

Alvarez, D., Alvarez, J.C., Gonzalez, R.C., Lopez, A.M., 2015. Upper limb joint angle measurement in occupational health. Comput Methods Biomech Biomed Engin, 1-12.
Bergamini, E., Ligorio, G., Summa, A., Vannozzi, G., Cappozzo, A., Sabatini, A.M., 2014. Estimating orientation using magnetic and inertial sensors and different sensor fusion approaches: accuracy assessment in manual and locomotion tasks. Sensors (Basel) 14, 18625-18649.
Cappozzo, A., Catani, F., Croce, U.D., Leardini, A., 1995. Position and orientation in space of bones during movement: anatomical frame definition and determination. Clin Biomech 10, 171-178.
de Vries, W.H.K., Veeger, H.E.J., Baten, C.T.M., van der Helm, F.C.T., 2009. Magnetic distortion in motion labs, implications for validating inertial magnetic sensors. Gait & posture 29, 535-541.
Faber, G.S., Chang, C.C., Rizun, P., Dennerlein, J.T., 2013. A novel method for assessing the 3-D orientation accuracy of inertial/magnetic sensors. Journal of Biomechanics 46, 2745-2751.
Gamage, S.S., Lasenby, J., 2002. New least squares solutions for estimating the average centre of rotation and the axis of rotation. J Biomech 35, 87-93.
Harrington, M.E., Zavatsky, A.B., Lawson, S.E., Yuan, Z., Theologis, T.N., 2007. Prediction of the hip joint centre in adults, children, and patients with cerebral palsy based on magnetic resonance imaging. J Biomech 40, 595-602.
Kainz, H., Carty, C.P., Modenese, L., Boyd, R.N., Lloyd, D.G., 2015. Estimation of the hip joint centre in human motion analysis: a systematic review. Clin Biomech 30, 319-329.
Kendell, C., Lemaire, E.D., 2009. Effect of mobility devices on orientation sensors that contain magnetometers. J Rehabil Res Dev 46, 957-962.
Kim, S., Nussbaum, M.A., 2013. Performance evaluation of a wearable inertial motion capture system for capturing physical exposures during manual material handling tasks. Ergonomics 56, 314-326.
Labaj, A., Diesbourg, T., Dumas, G., Plamondon, A., Mercheri, H., Larue, C., 2016. Posture and lifting exposures for daycare workers. International Journal of Industrial Ergonomics 54, 83-92.
Leardini, A., Chiari, L., Della Croce, U., Cappozzo, A., 2005. Human movement analysis using stereophotogrammetry. Part 3. Soft tissue artifact assessment and compensation. Gait & posture 21, 212-225.
Lebel, K., Boissy, P., Hamel, M., Duval, C., 2015. Inertial Measures of Motion for Clinical Biomechanics: Comparative Assessment of Accuracy under Controlled Conditions – Changes in Accuracy over Time. PLoS ONE 10, e0118361.
Mecheri, H., Robert-Lachaine, X., Larue, C., Plamondon, A., 2016. Evaluation of Eight Methods for Aligning Orientation of Two Coordinate Systems. J Biomech Eng 138.
Ohlendorf, D., Schwarzer, M., Rey, J., Hermanns, I., Nienhaus, A., Ellegast, R., Ditchen, D., Mache, S., Groneberg, D.A., 2015. Medical work assessment in German hospitals: a study protocol of a movement sequence analysis (MAGRO-MSA). J Occup Med Toxicol 10, 1.
Palermo, E., Rossi, S., Patane, F., Cappa, P., 2014. Experimental evaluation of indoor magnetic distortion effects on gait analysis performed with wearable inertial sensors. Physiol Meas 35, 399-415.
Plamondon, A., Delisle, A., Larue, C., Brouillette, D., McFadden, D., Desjardins, P., Lariviere, C., 2007. Evaluation of a hybrid system for three-dimensional measurement of trunk posture in motion. Applied Ergonomics 38, 697-712.

Prairie, J., Corbeil, P., 2014. Paramedics on the job: dynamic trunk motion assessment at the workplace. Appl Ergon 45, 895-903.
Reed, M., Manary, M.A., Schneider, L.W., 1999. Methods for measuring and representing automobile occupant posture. SAE Technical Paper.
Robert-Lachaine, X., Mecheri, H., Larue, C., Plamondon, A., 2016. Validation of inertial measurement units with an optoelectronic system for whole-body motion analysis. Med Biol Eng Comput (in press).
Robert-Lachaine, X., Mecheri, H., Larue, C., Plamondon, A., 2017. Accuracy and repeatability of single-pose calibration of inertial mesurement units for whole-body motion analysis. Gait & posture (in press).
Roetenberg, D., Baten, C., Veltink, P.H., 2007. Estimating body segment orientation by applying inertial and magnetic sensing near ferromagnetic materials. Neural Systems and Rehabilitation Engineering, IEEE Transactions on 15, 469-471.
Roetenberg, D., Luinge, H., Slycke, P., 2009. Xsens MVN: full 6DOF human motion tracking using miniature inertial sensors, Xsens Motion Technologies BV, Tech.Rep.
Roetenberg, D., Luinge, H.J., Baten, C.T., Veltink, P.H., 2005. Compensation of magnetic disturbances improves inertial and magnetic sensing of human body segment orientation. IEEE Trans Neural Syst Rehabil Eng 13, 395-405.
Schall, M.C., Jr., Fethke, N.B., Chen, H., Oyama, S., Douphrate, D.I., 2015. Accuracy and repeatability of an inertial measurement unit system for field-based occupational studies. Ergonomics, 1-23.
Schiefer, C., Ellegast, R.P., Hermanns, I., Kraus, T., Ochsmann, E., Larue, C., Plamondon, A., 2014. Optimization of inertial sensor-based motion capturing for magnetically distorted field applications. J Biomech Eng 136, 121008.
Wu, G., Siegler, S., Allard, P., Kirtley, C., Leardini, A., Rosenbaum, D., Whittle, M., D'Lima, D.D., Cristofolini, L., Witte, H., Schmid, O., Stokes, I., Standardization, Terminology Committee of the International Society of, B., 2002. ISB recommendation on definitions of joint coordinate system of various joints for the reporting of human joint motion--part I: ankle, hip, and spine. International Society of Biomechanics. J Biomech 35, 543-548.
Wu, G., van der Helm, F.C., Veeger, H.E., Makhsous, M., Van Roy, P., Anglin, C., Nagels, J., Karduna, A.R., McQuade, K., Wang, X., Werner, F.W., Buchholz, B., 2005. ISB recommendation on definitions of joint coordinate systems of various joints for the reporting of human joint motion--Part II: shoulder, elbow, wrist and hand. J Biomech 38, 981-992.